Published in final edited form as:
J Immunol. 2015 January 1; 194(1): 210–222. doi:10.4049/jimmunol.1402453.

β-Catenin Signaling Drives Differentiation and Proinflammatory Function of IRF8-Dependent Dendritic Cells

Sara B. Cohen[*], **Norah L. Smith**[*], **Courtney McDougal**[*], **Marion Pepper**[†], **Suhagi Shah**[‡], **George S. Yap**[‡], **Hans Acha-Orbea**[#], **Aimin Jiang**[¶], **Björn E. Clausen**[**], **Brian D. Rudd**[*], and **Eric Y. Denkers**[*]

[*]Department of Microbiology & Immunology, Cornell University College of Veterinary Medicine, Ithaca, NY USA 14867 [†]Department of Immunology, University of Washington School of Medicine, Seattle, WA 98101 USA [‡]Center for Immunity and Inflammation, New Jersey Medical School, Rutgers, The State University of New Jersey, Newark, NJ USA 07101 [¶]Department of Biochemistry, University of Lausanne, CH-1066, Epalinges, Switzerland [#]Department of Immunology, Roswell Park Cancer Institute, Buffalo, NY 14263 USA [**]Institute for Experimental Molecular Medicine, University Medical Center of Johannes Gutenberg-University Mainz, 55131, Mainz, Germany

Abstract

β-catenin signaling has recently been tied to the emergence of tolerogenic dendritic cells (DC). Here we demonstrate a novel role for β-catenin in directing DC subset development through IRF8 activation. We found that splenic DC precursors express β-catenin, and DC from mice with CD11c-specific constitutive β-catenin activation upregulated IRF8 through targeting of the *Irf8* promoter, leading to in vivo expansion of IRF8-dependent $CD8\alpha^+$, plasmacytoid, and $CD103^+CD11b^-$ DC. β-catenin-stabilized $CD8\alpha^+$ DC secreted elevated IL-12 upon in vitro microbial stimulation, and pharmacological β-catenin inhibition blocked this response in WT cells. Upon infections with *Toxoplasma gondii* and vaccinia virus, mice with stabilized DC β-catenin displayed abnormally high Th1 and $CD8^+$ T lymphocyte responses, respectively. Collectively, these results reveal a novel and unexpected function for β-catenin in programming DC differentiation towards subsets that orchestrate proinflammatory immunity to infection.

Introduction

Dendritic cells (DC) critically bridge innate and adaptive immunity through their exquisite capacity to drive antigen-specific T cell activation and effector subset differentiation. Furthermore, DC are central players in determining tolerance versus immunity during inflammation and infection (1). DC are a heterogeneous population of cells with varying surface markers and transcription factor requirements. All originate from a common myeloid progenitor (CMP), but they subsequently differentiate into distinct subsets, including monocyte-derived DC (moDC), conventional DC (cDC), and plasmacytoid DC (pDC).

Correspondence: Eric Y. Denkers, eyd1@cornell.edu, Phone: (607) 253-4022, Fax: (607) 253-3384.

Many elegant studies have identified phenotypic and functional differences amongst these subsets, but identifying factors determining control points of DC subset generation is a continuing focus of intense interest. Several key cytokines and transcription factors have been implicated in controlling DC developmental pathways (2), and recent gene mapping studies have begun to elucidate the order in which these factors become expressed (3, 4). For example, transcription factor Batf3 is involved in generation of splenic CD8α$^+$ DC, while IRF4 is important in differentiation of CD11b$^+$CD103$^+$ DC in the intestinal lamina propria (5, 6). Recently, Zbtb46 was identified as a global transcription factor necessary for generation of cDC(3). Nevertheless, a thorough understanding of the mechanisms of DC differentiation and the signals that direct branch points leading to distinct subsets remains incomplete.

β-catenin is the primary mediator of the Wnt signaling pathway and is critical for numerous cellular functions, including hematopoietic cell fate determination and proliferation (7, 8). Cytosolic β-catenin levels are normally maintained at low levels through continual phosphorylation by the serine threonine kinases glycogen synthase kinase (GSK)-3β and casein kinase (CK) I-α, which cooperate to promote its ubiquitination and proteosomal degradation. Activating Wnt ligands trigger disassembly of the complex that coordinates these kinases, leaving β-catenin unphosphorylated, in turn enabling nuclear translocation for transcriptional activity in association with T cell factor/lymphoid enhancer factor (Tcf/Lef) transcription factors (9). While normally associated with embryonic development and tumorigenesis (10), β-catenin is increasingly being recognized for its role in immunity (11). This is particularly the case for DC, where β-catenin signaling was first implicated in cluster disruption-mediated maturation towards a tolerogenic phenotype during in vitro culture (12). Moreover, β-catenin was found to be involved in the generation or maintenance of tolerogenic DC subsets in the intestinal mucosa (13).

Here, we provide surprising new insight into the role of β-catenin in DC function by employing transgenic mice with a CD11c-specific deletion in the third exon of the β-catenin gene. The exon 3 fragment encodes the β-catenin amino acid sequence that is targeted for GSK-3β-mediated serine threonine phosphorylation and subsequent degradation. Removal of this region through Cre-lox mediated excision therefore results in phosphorylation-resistant and constitutively active β-catenin (14). We made the unexpected discovery that β-catenin stabilization in DC results in selective expansion of steady-state levels of splenic CD8α$^+$ DC, pDC, and peripheral CD103$^+$ DC. These DC subsets share a dependence on IRF8 for their differentiation, and in accordance with this observation, we show that constitutive β-catenin signaling increases IRF8 expression by these DC subsets via enhanced targeting of the *Irf8* promoter. We employed infections with the intracellular protozoan *Toxoplasma gondii* and vaccinia virus to determine the in vivo consequences of DC-specific β-catenin stabilization. In accord with the known role of CD8α$^+$ DC as an IL-12 source and driver of Th1 responses during *T. gondii* infection (15), the parasite triggered an abnormally strong Th1 response associated with overproduction of IL-12 and IFN-γ. Immunity to vaccinia virus is known to require a DC-mediated cross-presentation pathway (16). As such, vaccinia infection in mutant mice triggered enhanced expansion and activation of virus-specific CD8$^+$ T cells. Our results uncover a new role for β-catenin in controlling IRF8

expression in DC, thereby revealing this transcription factor as a key player regulating IRF8-driven DC differentiation and proinflammatory function.

Materials and Methods

Ethics statement

All experiments in this study were performed strictly according to the recommendations of the Guide for the Care and Use of Laboratory Animals of the National Institutes of Health. The protocols were approved by the Institutional Animal Care and Use Committee at Cornell University (permit number 1995–0057). All efforts were made to minimize animal suffering during the course of these studies.

Mice and infections

Female Swiss Webster mice (6–8 weeks of age) were purchased from the Jackson Laboratory (Bar Harbor, ME), and female C57BL/6 were purchased from Taconic Farms (Germantown, NY). C57BL/6-Tg (TcraTcrb)425Cbn/J (OT-II) mice were obtained from the Jackson Laboratory and maintained as a breeding colony at Cornell University College of Veterinary Medicine. The β-catenin $Ex3^{fl/fl}$ mice were kindly provided by M. M. Taketo (Kyoto University) and were maintained as breeding colonies crossed to CD11c-cre expressing mice at the Transgenic Mouse Core Facility at the Cornell University College of Veterinary Medicine. Cre^+ offspring ($Ex3^{DC-/-}$ mice) were identified by PCR amplification of the *Cre* gene from genomic DNA isolated from tail snips. Infections were initiated in 8–12 week old mice. *T. gondii* infections were performed by intraperitoneal inoculation of 25 cysts of the type II ME49 strain. Cysts were isolated from chronically infected Swiss Webster mice by homogenization of whole brain in sterile PBS. Alternatively, mice were inoculated with 2×10^5 pfu of recombinant vaccinia virus expressing MHCI-restricted HSV $gB_{498\text{-}505}$ (VACV-gB) by intraperitoneal injection (17). VACV-gB was maintained in 143B cells for the generation of viral stocks.

Preparation and purification of leukocytes

Splenocyte single cell suspensions were prepared by crushing spleens between sterile glass slides and filtering the resulting suspension through 40 μM filters. For lung leukocytes, lung tissue was minced with sterile razor blades and incubated with collagenase type IV (Sigma) in a 37°C water bath for 30 min with frequent agitation. The resulting digest was passed through a 40-μM filter to create a single cell suspension. A single round of positive selection using $CD11c^+$ magnetic bead sorting was performed for purification of total splenic DC from single cell suspensions (Stem Cell Technologies), while two-step magnetic bead sorting, with an initial negative selection to enrich for DC followed by $CD8\alpha^+$ positive selection (Miltenyi Biotec), was performed to isolate $CD8\alpha^+$ splenic DC.

In vitro culture of bone marrow-derived DC and MutuDC1940 cells

Bone marrow-derived DC were cultured as described previously (18). Briefly, femurs of $Ex3^{fl/fl}$, $Ex3^{DC-/-}$, or C57BL/6 mice were flushed with PBS and cultured for 9 days in media containing 10% fetal calf serum (Hyclone), 100 U/ml penicillin (Life Technologies), 0.1 mg/ml streptomycin (Life Technologies), 50 μM 2-mercaptoethanol (Sigma), and 20

ng/ml GM-CSF (Peprotech). Cells were harvested from the plates with gentle pipetting and cultured as indicated. Flt3L BMDC cultures were performed by flushing femurs with PBS, lysing red blood cells with ACK lysis buffer (Life Technologies), and plating cells in RPMI supplemented with 10% fetal calf serum, 25 mM HEPES (Life Technologies), 100 U/ml penicillin (Life Technologies), 0.1 mg/ml streptomycin (Life Technologies), and 100 ng/ml murine Flt3L (Peprotech). Cells were cultured for 9 days at 37°C. MutuDC1940 cells, kindly provided by Dr. Hans Acha-Orbea (University of Lausenne), were grown in a monolayer in media containing 8% fetal calf serum (Hyclone), 10 mM HEPES (Life Technologies), 50 μM 2-mercaptoethanol, 100 U/ml penicillin (Life Technologies), and 0.1 mg/ml streptomycin (Life Technologies). Cells were harvested by 10 min incubation with PBS and 5 mM EDTA.

Western blotting

To validate nuclear translocation of β-catenin in $Ex3^{DC-/-}$ mice, BMDC were subjected to nuclear and cytoplasmic fractionation following the manufacturer's guidelines (Active Motif). Resulting nuclear and cytoplasmic proteins were diluted in reducing SDS sample buffer and separated by 10% SDS-PAGE. Separated proteins were transferred onto nitrocellulose and blocked for 1 hr at room temperature in Tris-buffered saline containing 0.1% Tween-20 and 5% nonfat dry milk (TBST). Following 3 washes in TBST, blots were incubated overnight in primary antibody diluted in TBST containing 5% BSA. Blots were subsequently washed in TBST and incubated for 1 hr with anti-rabbit IgG conjugated to horseradish peroxidase-conjugated (HRP) diluted in TBST containing 5% nonfat dry milk. Following 5 washes in TBST, blots were developed and imaged using a chemiluminescent detection system (Thermo Scientific). Anti-β-catenin and anti-PARP were purchased from Cell Signaling, and anti-Rab5a was purchased from Santa Cruz Biotechnology.

Flow cytometry

Single cell suspensions were washed in PBS prior to resuspension in Zombie Aqua viability dye (BioLegend) for 15 min at room temperature to exclude dead cells. Primary antibodies (anti-CD11c FITC, eFluor610, or APC; anti-CD8α Pacific Blue or APC-Cy7; anti-CD4 PerCP-Cy5.5 or FITC; anti-PDCA-1 APC or PE; anti-NK1.1 FITC or APC; anti-CD11b FITC or APC-Cy7; anti-CD24 Pacific Blue; anti-CD103 PE; anti-B220 PE; anti-CD3 FITC; anti-Gr1 FITC; anti-CD127 PerCP-Cy5.5; anti-CD16/32 eFluor450; anti-CD19 FITC; anti-CD135 PE; anti-Sca1 PE-Cy7; anti-CD117 APC-Cy7; anti-MHCII PE or FITC) resuspended in ice-cold FACS buffer (1% bovine serum albumin/0.01% NaN_3 in PBS) were added directly to the cells for 30 min. Tetramer staining for $Tgd057^+CD8^+$ T cells (provided by George Yap, New Jersey School of Medicine and Dentistry), $CD4Ag28m^+CD4^+$ T cells (provided by Marion Pepper, University of Washington), and gB-8p:$K^{b+}CD8^+$ T cells (NIH Tetramer Core Facility, Emory University) was performed by labeling at room temperature for 1 hour. For intracellular staining, cells were fixed using the FoxP3/transcription factor staining kit fixative (eBioscience) and subsequently incubated with primary antibodies resuspended in the FoxP3/transcription factor permeabilization buffer (eBioscience). Antibodies used for intracellular cytokine staining include anti-IRF8 PerCP, and anti-IRF4 eFluor450 (eBioscience); anti-β-catenin Alexa-647 (Cell Signaling). IgG isotype controls (eBioscience) were used for each fluorophore. For IFN-γ staining following *T. gondii*

infection, cells were incubated for 4 hr with Brefeldin-A (eBioscience; 10 ug/ml), PMA (Sigma; 10 ng/ml), and ionomycin (Sigma; 1 ug/ml), while for VACV-gB infection, splenocytes were restimulated with gB-8p peptide (SSIEFARL; 10^{-7} M) for 5 hr in the presence of Brefeldin-A. Cells were then fixed with the FoxP3/transcription factor staining kit fixative (eBioscience) and subsequently incubated with anti-IFN-γ (PE-Cy7, BioLegend; PE, eBioscience). All samples were run on an LSRII flow cytometer (BD), and the data were analyzed using FlowJo software (FlowJo, Ashland, OR).

Identification of bone marrow and splenic DC progenitors

Bone marrow was flushed from the femur and tibia of $Ex3^{fl/fl}$ and $Ex3^{DC-/-}$ mice and broken up with a 21-gauge syringe. Bone marrow and splenocyte pellets were lysed with ACK buffer and passed through a 40-μm filter to generate single cell suspensions. For precursor staining, a FITC lineage cocktail was created in-house (anti-NK1.1, anti-CD11b, anti-Gr1, anti-Ter119, anti-CD3, anti-MHCII, anti-CD19). Gating strategies were adopted from a previous study (3), whereby CMP were defined as $Lin^{-}Sca1^{-}CD127^{-}CD117^{hi}CD11c^{-}CD135^{+}CD16/32^{-}$, GMP as $Lin^{-}Sca1^{-}CD127^{-}CD117^{hi}CD11c^{-}CD135^{-}CD16/32^{+}$, CDP as $Lin^{-}Sca1^{-}CD127^{-}CD117^{int}CD11c^{-}CD135^{+}CD16/32^{-}$, and pre-cDC as $Lin^{-}Sca1^{-}CD127^{-}CD117^{lo}CD16/32^{-}CD11c^{+}CD135^{+}$. Pre-$CD8\alpha^{+}$ DC were defined as $CD11c^{+}CD8\alpha^{-}B220^{-}CD24^{+}$ as previously described (19).

Chromatin immunoprecipitation

Recombinant murine Flt3 ligand bone marrow cultures from $Ex3^{DC-/-}$ mice (1×10^{7}) were cross-linked with 1% formaldehyde (Pierce) at room temperature for 6 min, and chromatin/protein complexes were prepared following the manufacturer's instructions (Millipore). Shearing was performed using a Bioruptor UCD-200 sonicator (Life Technologies) in an ice slurry, with a program of 30 seconds on and 60 seconds off for 30 min. Protein immunoprecipitation was performed overnight with agitation at 4°C using protein G magnetic beads and 2 μg of a rabbit monoclonal β-catenin antibody or rabbit IgG (Cell Signaling). The following day, samples were proteinase K digested at 65°C to free the DNA, and semi-quantitative PCR was performed to amplify a region of the *Irf8* promoter containing a Wnt/β-catenin binding site (Forward, CACACTGGGTGGACATTTG; Reverse, ACCTTATAAGCGTATGCAGATT). DNA levels were normalized to 1% input chromatin.

ICG-001 inhibition

BMDC (1×10^{6}) or MutuDC1940 cells (2×10^{5}) were plated and cultured overnight. The following day, the cells were cultured with 5 or 20 μM ICG-001 (Selleck Chemicals), respectively, or DMSO control for 5 hr or overnight at 37°C. Cells were surface stained for CD11c and/or CD24, fixed, intracellularly stained for IRF8, IRF4, and β-catenin, and analyzed by flow cytometry. Alternatively, DC were resuspended in Trizol (Life Technologies) for quantitative PCR analysis of *Irf8* and *Axin2* mRNA transcripts.

Measurement of mRNA by quantitative PCR

RNA was isolated from $CD11c^+$ splenocytes magnetically sorted from naïve $Ex3^{DC-/-}$ and $Ex3^{fl/fl}$ mice or from BMDC by resuspension in Trizol reagent (Life Technologies). RNA was converted to cDNA (Quanta Biosciences, Gaithersburg, MD) and assayed for gene expression by SYBR green technology (Quanta Biosciences). Primers were designed to span exons by Integrated DNA Technologies. The following primer sequences were used: *Irf8* Forward, TGCCACTGGTGACCGGATAT; Reverse, GACCATCTGGGAGAAAGCTGAA; *Nfil3* Forward, GAACTCTGCCTTAGCTGAGGT; Reverse, ATTCCCGTTTTCTCCGACACG; *Id2* Forward, ATGAAAGCCTTCAGTCCGGTG; Reverse, AGCAGACTCATCGGGTCGT; *Batf3* Forward, CAGACCCAGAAGGCTGACAAG; Reverse, CTGCGCAGCACAGAGTTCTC; *Axin2* Forward, TAGGTTCCGGCTATGTCTTTG; Reverse, TGTTTCTTACTCCCCATGCG. GAPDH was used as a housekeeping gene. Gene expression was normalized to $Ex3^{fl/fl}$ samples or DMSO controls.

Cytokine measurement

IFN-γ IL-12p70 and TNF-α secretion were assayed by enzyme-linked immunosorbent assay (ELISA) following the manufacturer's instructions (eBioscience) following culture with media, LPS (100 n/gml), or soluble tachyzoite antigen (50 μg/ml) prepared as previously described (20). IL-12p40 secretion was measured using an in-house ELISA(21).

Parasite burden measurement

Levels of *T. gondii* DNA were measured as described previously (22). Briefly, spleens were homogenized, and DNA was extracted using a tissue extraction kit (Omega Biotech). The *T. gondii* B1 gene and the host argininosuccinate lyase (ASL) gene were amplified by quantitative real-time PCR, and resulting ct values were compared to standard curves developed from 10-fold serial dilutions of parasite DNA and splenocyte DNA, respectively. The parasite burden is displayed as the ratio of *T. gondii* DNA to host DNA.

Statistical analyses

Differences between groups were analyzed by Student's *t* test. Expression of β-catenin among splenic DC subsets was analyzed by one-way ANOVA followed by a Newman-Keuls post-test. A Kaplan-Meier curve (Logrank test) was used to calculate differences in survival between $Ex3^{fl/fl}$ and $Ex3^{DC-/-}$ mice. P values were considered statistically significant at <0.05 and were designated *, $p<0.05$; **, $p<0.01$; *** $p<0.001$.

Results

β-catenin is selectively enriched in splenic DC precursors and mature DC

Common myeloid progenitors, (CMP), granulocyte-macrophage progenitors (GMP), common dendritic progenitors (CDP), and pre-conventional dendritic cells (pre-cDC) represent different stages of hematopoiesis towards the dendritic cell (DC) lineage and can be distinguished by surface marker expression (Supplemental Fig. 1) (3, 23). While CMP can develop into any cell of the myeloid lineage and GMP can ultimately become

macrophages, granulocytes, or DC, CDP and pre-cDC are restricted to the DC lineage, although they remain immature until terminal differentiation within the tissue (23). To investigate the role of β-catenin at these different stages of DC differentiation, β-catenin expression levels were determined among DC precursor populations in the bone marrow and spleens of wild-type (WT) mice by flow cytometry. We were able to detect each precursor population in both tissues, although the overall levels of precursors, particularly CDP, were far lower in the spleen (Supplemental Fig. 1). Interestingly, β-catenin was undetectable in the precursor populations in the bone marrow and in splenic CMP. However, β-catenin expression was increased in splenic GMP, CDP, and pre-cDC with GMP and pre-cDC displaying the highest levels (Fig. 1A, 1B). These results provide evidence that the β-catenin signaling axis may be active in later stages of DC development.

To ask if β-catenin expression was maintained in mature tissue-resident DC, levels were measured in splenic conventional DC (cDC) subsets and plasmacytoid DC (pDC). Compared to the $CD4^+$ splenic cDC subset, immediate $CD8\alpha^+$ DC precursors (pre-$CD8\alpha^+$ DC), which are defined by CD24 expression (19), $CD8\alpha^+$ DC, and pDC were all significantly enriched for β-catenin expression, where pre-$CD8\alpha^+$ DC and pDC expressed the highest levels (Fig. 1C, 1D). These data demonstrate that β-catenin is selectively induced in particular DC subsets and that, based upon protein expression levels, β-catenin signaling is more active in tissue-resident DC progenitors and mature DC than in bone marrow cells.

β-catenin stabilization directs splenic DC progenitors towards $CD8\alpha^+$ DC

Because β-catenin was clearly expressed by DC progenitors, we next investigated the effect of β-catenin stabilization on the outcome of DC differentiation. To address this, mice floxed for exon 3 of the β-catenin gene were crossed with CD11c-cre animals, resulting in Cre-positive progeny whose $CD11c^+$ cells possessed an exon 3-deleted β-catenin form resistant to phosphorylation-induced degradation (14). Flow cytometric analysis of $CD11c^+$ splenic DC from Cre-positive offspring ($Ex3^{DC-/-}$ mice) demonstrated high β-catenin expression levels compared to Cre-negative littermate controls ($Ex3^{fl/fl}$ mice), indicating accumulation of β-catenin protein upon exon 3 deletion (Fig. 2A). This was confirmed to be specific to $CD11c^+$ cells, as $CD4^+$ T cells from $Ex3^{DC-/-}$ mice did not display upregulation of β-catenin compared to $CD4^+$ T cells from $Ex3^{fl/fl}$ mice (Fig. 2B). Furthermore, upon cytoplasmic and nuclear fractionation, $Ex3^{DC-/-}$ BMDC were found to be enriched for a truncated form of nuclear β-catenin compared to $Ex3^{fl/fl}$ DC, confirming enhanced nuclear translocation of protein (Fig. 2C). Thus, CD11c-directed exon 3 deletion results in β-catenin accumulation and nuclear translocation.

To determine the effect of β-catenin stabilization on DC precursor levels, bone marrow and splenic pre-cDC were quantified from $Ex3^{fl/fl}$ and $Ex3^{DC-/-}$ mice by flow cytometry. Consistent with the failure to detect β-catenin in bone marrow precursors (Fig. 1B), no differences were observed in the levels of DC progenitors in the bone marrow following β-catenin stabilization (Fig. 2D). However, β-catenin stabilization in $Ex3^{DC-/-}$ mice led to significantly fewer splenic pre-cDC compared to $Ex3^{fl/fl}$ littermate controls (Fig. 2E), suggesting that constitutive β-catenin signaling was depleting this precursor pool. We next asked whether this decrease in progenitors influenced later stages of DC development, in

particular by quantifying levels of pre-CD8α$^+$ DC. Indeed, DC-specific β-catenin activation resulted in a 2-fold increase in splenic pre-CD8β$^+$ DC compared to WT controls (Fig. 2F). These data suggest that β-catenin signaling drives the differentiation of splenic DC progenitors into the immediate precursors of mature CD8β$^+$ DC.

β-catenin stabilization expands splenic and peripheral dendritic cell populations

Since β-catenin signaling influenced the levels of splenic DC progenitors, we next focused on the outcome of β-catenin stabilization on steady-state levels of mature tissue-resident DC. We first observed that the percentage and total number of CD11c$^+$MHCII$^+$ cells were unaffected in Ex3$^{DC-/-}$ mice (Fig. 3A, 3B). However, further analysis revealed a striking expansion of the CD8α$^+$ DC subset and a concomitant decrease in CD11b$^+$ DC (Fig. 3C, 3E). Furthermore, plasmacytoid DC (pDC), as defined by expression of B220 and PDCA-1, were also expanded in the spleens of Ex3$^{DC-/-}$ mice (Fig. 3F, 3G). These collective data suggest that β-catenin exerts major effects on the generation of specific splenic DC populations and are consistent with the finding that these particular subsets upregulate β-catenin during development (Fig. 1D).

Peripheral DC can be subdivided into CD103$^+$CD11b$^-$, CD103$^+$CD11b$^+$, and CD103$^-$CD11b$^+$ DC and, much like splenic DC subsets, these DC display differential transcription factor requirements and functions (6, 24). Importantly, CD103$^+$CD11b$^-$ DC found in non-lymphoid tissues, such as the intestine and the lung, exhibit a similar dependence upon Batf3 as the CD8α$^+$ DC subset, leading to the conclusion that these two subsets are developmentally related (24). Examination of these DC subsets in Ex3$^{DC-/-}$ mice revealed a dramatic expansion of resident lung CD103$^+$CD11b$^-$ DC compared to Ex3$^{fl/fl}$ littermate controls (Fig. 3H, 3I). Furthermore, intestinal CD103$^+$CD11b$^-$ DC, but not CD103$^+$CD11b$^+$ DC, were also expanded in Ex3$^{DC-/-}$ mice (Fig. 3J–L). These data demonstrate that constitutive DC β-catenin signaling promotes a developmental pathway that is shared by splenic CD8α$^+$ DC, pDC and peripheral CD103$^+$ DC.

β-catenin signaling controls Irf8 expression

Genetic knockout studies have identified several transcription factors involved in CD8α DC differentiation, including *Id2*, *Nfil3*, *Batf3*, and *Irf8* (5, 25–27). Therefore, we determined expression levels of these transcription factors amongst splenic CD11c$^+$ cells from Ex3$^{fl/fl}$ and Ex3$^{DC-/-}$ mice. While there was no significant difference in *Id2* expression, *Nfil3* and *Batf3* transcripts were slightly increased albeit in a statistically non-significant manner (Fig. 4A). However, there was a striking increase in *Irf8* expression in the CD11c compartment upon β-catenin stabilization (Fig. 4A). We also assessed IRF8 protein expression in CD8α$^-$ and CD8α$^+$ splenic DC in Ex3$^{fl/fl}$ and Ex3$^{DC-/-}$ mice by flow cytometry. Levels of IRF8 were relatively low in CD8α$^-$ DC from both mouse strains (Fig. 4B, 4C). However, there was an increase in IRF8 mean fluorescence intensity (MFI) in CD8α$^+$ DC in both mouse strains. Furthermore, IRF8 MFI and percent positive populations were increased when comparing CD8α$^+$ DC from Ex3$^{DC-/-}$ relative to Ex3$^{fl/fl}$ strains (Fig. 4B–D). To confirm that the effect of β-catenin stabilization was specific for IRF8, we examined expression of IRF4 and found it to be unchanged in Ex3$^{DC-/-}$ relative to Ex3$^{fl/fl}$ CD8α splenic DC (Fig. 4E). Consistent with this finding, levels of splenic CD4$^+$ DC and intestinal CD11b$^+$CD103$^+$

DC, both of which are known to depend on IRF4 for development, were unchanged between $Ex3^{fl/fl}$ and $Ex3^{DC-/-}$ mice (6, 26) (Fig. 3J, 3L; data not shown).

To ask whether β-catenin targets the *Irf8* promoter in vivo, chromatin immunoprecipitation assays were performed on Flt3 ligand cultures of bone marrow DC derived from $Ex3^{DC-/-}$ mice. β-catenin displayed a greater than 6-fold enrichment in *Irf8* promoter occupancy over IgG control, suggesting a direct role for this signaling axis in *Irf8* transcription (Fig. 4F). To ask if *Irf8* transcription could be blocked by inhibiting β-catenin, WT BMDC were cultured with the Wnt/β-catenin inhibitor ICG-001, which competes with β-catenin for binding to its co-factor Creb-binding protein (CBP)(28). As a control, 5 hr of ICG-001 treatment led to a significant reduction in transcript levels of the known β-catenin target gene *Axin2*(29). Importantly, *Irf8* transcripts were also significantly reduced following ICG-001 treatment (Fig. 4G). This downregulation was observed at the protein level, as IRF8 expression in BMDC was markedly decreased compared to DMSO-treated control cells by flow cytometry (Fig. 4H). Furthermore, ICG- 001 treatment of MutuDC1940 cells, a DC-derived cell line that has many characteristics of $CD8\alpha^+$ DC(30), also resulted in strong downregulation of IRF8 (Fig. 4I). IRF4 levels were unchanged by ICG-001 treatment, confirming the specificity of β-catenin signaling for IRF8 (data not shown). These data establish a functional link between β-catenin and IRF8 expression that controls differentiation of $CD8\alpha^+$ DC, pDC and peripheral $CD103^+$ DC.

β-catenin stabilization enhances IL-12 production by $CD8\alpha^+$ DC

$CD8\alpha^+$ DC are a potent IL-12 source during infection with the Th1 pathogen *Toxoplasma gondii* (15). Furthermore, it was recently shown that this cytokine activity requires IRF8(31). Additionally, LPS has been shown to upregulate *Irf8* expression, resulting in binding to the IL-12 promoter (32). Therefore, we wanted to determine if increased IRF8 expression in $CD8\alpha^+$ DC from $Ex3^{DC-/-}$ mice would impact their functional activity, in particular as related to IL-12 production.

To examine this, whole splenocytes from $Ex3^{fl/fl}$ and $Ex3^{DC-/-}$ mice were cultured in the presence of media, LPS, or soluble tachyzoite antigen (STAg), an antigenic preparation of *T. gondii* that stimulates $CD8\alpha^+$ DC IL-12 through the interaction between TLR11/12 and parasite profilin (31). Indeed, upon LPS or STAg stimulation, supernatants from $Ex3^{DC-/-}$ splenocytes contained significantly increased levels of IL-12p40 compared to $Ex3^{fl/fl}$ controls (Fig. 5A). To confirm that the source of IL-12 was DC, $CD11c^+$ cells were magnetically purified (~90% purity) from $Ex3^{fl/fl}$ and $Ex3^{DC-/-}$ splenocytes and cultured with LPS and STAg. As expected, increased IL-12 secretion was again observed in $Ex3^{DC-/-}$ cells (Fig. 5B). These results clearly show that DC from $Ex3^{DC-/-}$ produce more IL-12 than cells from WT littermates. However, they leave open to question whether this is a result of an increase in the proportion of $CD8\alpha^+$ DC, or whether $Ex3^{DC-/-}$ $CD8\alpha^+$ DC produce increased IL-12 on a cell-to-cell basis relative to corresponding cells from $Ex3^{fl/fl}$ mice. Therefore, $CD8\alpha^+$ and $CD8\alpha^-$ DC were magnetically purified from $Ex3^{fl/fl}$ and $Ex3^{DC-/-}$ spleens and stimulated in vitro with STAg. While IL-12 production was restricted to the $CD8\alpha^+$ subset, the $Ex3^{DC-/-}$ $CD8\alpha^+$ DC secreted enhanced IL-12 levels compared to $Ex3^{fl/fl}$ $CD8\alpha^+$ DC (Fig. 5C). Next, WT splenocytes were treated with the β-catenin

inhibitor ICG-001 and then stimulated with STAg or LPS overnight. Inhibitor-treated cells secreted lower levels of IL-12p40 compared to DMSO-treated cells without negatively affecting viability (Fig. 5D, data not shown). Furthermore, the elevated IL-12 secretion displayed by $Ex3^{DC-/-}$ splenocytes over $Ex3^{fl/fl}$ splenocytes could be inhibited by treatment with ICG-001, further indicating that ICG-001 treatment suppresses β-catenin-dependent responses (Fig. 5E). To further implicate $CD8\alpha^+$ DC in these findings, we replicated these experiments in vitro using MutuDC1940 cells. Stimulation of MutuDC1940 cells with STAg resulted in extremely high IL-12 levels, consistent with their origin from splenic $CD8\alpha^+$ DC. Furthermore, pre-treatment of MutuDC1940 cells with ICG-001 significantly impaired the IL-12 response to STAg (Fig. 5F). Thus, β-catenin stabilization promotes both differentiation and IL-12-secreting capacity of $CD8\alpha^+$ DC by promoting increased *Irf8* expression.

Constitutive DC β-catenin signaling promotes Th1 immunity during Toxoplasma gondii infection

As a source of IL-12 that drives Th1 activation, CD8α DC are required to control infection with *Toxoplasma*, yet overexpression of IL-12 and downstream proinflammatory cytokines is also lethal (15, 33). Therefore, we used intraperitoneal infection with *T. gondii* to evaluate the impact of DC β-catenin stabilization on host immunity. $Ex3^{DC-/-}$ mice began to succumb within 9 days of low dose *T. gondii* intraperitoneal infection, while the $Ex3^{fl/fl}$ littermate controls fully survived acute infection (Fig. 6A). Parasite levels in the spleen (Fig. 6B) and peritoneal cavity (data not shown) were equivalent between the genotypes, arguing that susceptibility of $Ex3^{DC-/-}$ mice was not due to defective control of *Toxoplasma*.

Splenic DC from infected $Ex3^{DC-/-}$ mice secreted dramatically more IL-12 compared to $Ex3^{fl/fl}$ controls as measured by both p40 (Fig. 6C) and p70 (Fig. 6D) subunits and, at nearly 50 ng/ml, the level of IL-12p40 detected in $Ex3^{DC-/-}$ mice was approximately 5-fold over WT controls. To examine Th1 responses in these animals, $Ex3^{fl/fl}$ and $Ex3^{DC-/-}$ splenocytes from infected mice were cultured in vitro, and the supernatants were assayed for both IL-12 and IFN-γ. Accompanying increased IL-12 secretion by $Ex3^{DC-/-}$ splenocytes, IFN-γ levels were enhanced, suggesting elevated T and possibly NK cell activation in $Ex3^{DC-/-}$ mice in response to *T. gondii* infection (Fig. 6E). Furthermore, serum collected from infected mice revealed significantly elevated levels of IFN-γ, IL-12, and TNF-α in $Ex3^{DC-/-}$ mice compared to $Ex3^{fl/fl}$ controls (Fig. 6F), suggesting systemic hyperproduction of proinflammatory cytokines upon DC β-catenin stabilization. By contrast, IL-17 was undetectable or expressed at very low levels in splenocyte cultures or serum prepared from infected $Ex3^{fl/fl}$ or $Ex3^{DC-/-}$ mice (data not shown).

To determine the source of elevated Th1 cytokines in $Ex3^{DC-/-}$ mice during *T. gondii* infection, IFN-γ production by splenic $CD4^+$ T cells, $CD8^+$ T cells, and natural killer (NK) cells was assayed 8 days post-infection. Both $CD4^+$ T cells and NK cell populations in $Ex3^{DC-/-}$ mice displayed a marked increase in IFN-γ responses compared to $Ex3^{fl/fl}$ littermate controls (Fig. 7A, 7C). Interestingly, given previous studies implicating $CD8\alpha^+$ DC in cross-presentation (5, 34), IFN-γ from $CD8^+$ T cells was not significantly changed between the two genotypes (Fig. 7B).

We next determined whether the increase in IFN-γ could be explained by increased activation and expansion of *Toxoplasma*-specific T cells. We used MHCI tetramers that bind $CD8^+$ T lymphocytes specific for the endogenous *T. gondii* epitope Tgd057 and MHCII tetramers that bind $CD4^+$ T cells specific for the *Toxoplasma* epitope CD4Ag28m (35, 36). The frequency of parasite-specific $CD4^+$ and $CD8^+$ T cells was equivalent in $Ex3^{DC-/-}$ and $Ex3^{fl/fl}$ mice (Fig. 7D, 7E). Although IFN-γ produced by antigen-specific $CD8^+$ T cells was equivalent in $Ex3^{fl/fl}$ and $Ex3^{DC-/-}$ mice, levels of cytokine produced by tetramer-positive $CD4^+$ T lymphocytes were increased in $Ex3^{DC-/-}$ relative to $Ex3^{fl/fl}$ mice (Fig. 7F, 7G). Therefore, in the context of *T. gondii* infection, DC β-catenin stabilization impacts the intensity of the CD4 and NK cell IFN-γ response, but does not have a measurable influence on IFN-γ production by $CD8^+$ T cells.

DC β-catenin signaling enhances $CD8^+$ T cell priming during vaccinia virus infection

DC-mediated cross-presentation of exogenous antigen through the cytosolic pathway is crucial for the generation of a $CD8^+$ T cell response against vaccinia virus (VACV) infection (16, 37). Thus, we finally asked if DC β-catenin signaling influenced DC cross-presentation in the context of VACV infection. To address this, $Ex3^{fl/fl}$ and $Ex3^{DC-/-}$ mice were infected intraperitoneally with recombinant VACV expressing the herpes simplex virus (HSV) glycoprotein B (gB) peptide (VACV-gB)(17). On day 6 post-infection, spleens were harvested, and gB-specific $CD8^+$ T cells were quantified by flow cytometry using MHCI-restricted gB-8p:K^b tetramers. We found a striking increase in the percentage and total number of gB-specific $CD8^+$ T cells in $Ex3^{DC-/-}$ mice compared to littermate controls, suggesting increased cross-presentation by β-catenin-stabilized DC (Fig. 8A–C). Furthermore, restimulation of splenocytes with gB peptide revealed significantly increased IFN-γ^+CD8^+ T cells in $Ex3^{DC-/-}$ mice, demonstrating a functional impact of DC β-catenin activation on $CD8^+$ T cell activity (Fig. 8D–F). These results demonstrate that stabilization of DC β-catenin promotes development of $CD8^+$ T cell responses in the context of viral infection.

Discussion

Dendritic cell differentiation is a complex process involving an array of transcription factors and growth factor cytokines whose details are continuing to be elucidated. In this study we identify an unexpected role for β-catenin in controlling differentiation of $CD8\alpha^+$ DC, pDC, and developmentally related non-lymphoid $CD103^+$ DC. This pattern of transcriptional control precisely matches that of IRF8(24, 26, 38). In support of a functional connection between β-catenin and IRF8, overexpression of β-catenin increased steady state IRF8 levels in $CD8\alpha^+$ DC. In addition, IL-12 production by $CD8\alpha^+$ DC, a known function of this cell subset, was prevented by β-catenin inhibition concomitant with IRF8 down-modulation, and $CD8\alpha^+$ DC overexpressing β-catenin produced enhanced IL-12 in response to microbial stimulation. During infection with *T. gondii*, a prototypic Type 1-inducing pathogen, mice overexpressing DC-specific β-catenin developed exacerbated Th1 responses culminating in early death. In addition, infection with VACV increased expansion and IFN-γ production by virus-specific $CD8^+$ T lymphocytes.

Wnt/β-catenin signaling has a well-studied role in embryogenesis and tumorigenesis (10). It is now also clear that differentiation of T cells and NK cells requires LEF-1/TCF β-catenin cofactors. Furthermore, β-catenin regulates proliferation of pro-B cells (39). Using a β-catenin stabilization approach similar to that employed here, it has been found that this signaling molecule plays a fundamental role in regulating hematopoietic stem cells in the bone marrow (40). Furthermore, β-catenin has been recently shown to target *Irf8* during hematopoiesis to alter granulocyte development (41). We now show that stabilization of β-catenin at the CD11c-expressing stage has unanticipated effects on generation of mature DC subsets whose differentiation depends upon IRF8.

Our data are notable because other recent studies have implicated β-catenin signaling in promoting tolerogenic DC phenotypes. For example, in contrast to activation by microbial stimulation, cluster disruption of bone marrow-derived DC activates β-catenin, endowing the cells with the ability to promote regulatory T cells that protect against experimental autoimmune encephalitis (EAE)(12). In the intestine, β-catenin expression by $CD11c^+$ cells was shown to be required for regulatory T cell induction and production of anti-inflammatory factors, including retinoic acid-metabolizing enzymes, TGF-β and IL-10 (13). In this case, absence of β-catenin in DC increased sensitivity to dextran sodium sulfate (DSS)-mediated colitis. Our data uncover an important new facet of β-catenin signaling because they reveal a role in promoting the differentiation of IRF8-dependent $CD8\alpha^+$ DC with enhanced proinflammatory activity.

IRF8 controls conventional DC formation by actively suppressing granulocyte differentiation while simultaneously promoting commitment to the DC lineage (42, 43). This is best illustrated by the observation that IRF8-deficient mice suffer from chronic myeloid leukemia-like syndrome with massive expansion of granulocytic cells (44). As such, IRF8 expression is enriched in CDP over common myeloid progenitors and is nearly absent in GMP(43), which is consistent with our finding that splenic DC precursors express β-catenin. Mice expressing constitutive β-catenin in the hematopoietic stem cell compartment, either through exon 3 deletion or transgenic expression of a phosphorylation resistant β-catenin, display a differentiation block at the granulocyte progenitor stage, which leads to lethality of the host (40, 45). It is tempting to speculate, therefore, that over-activation of β-catenin may lead to excessive IRF8 expression as early as the progenitor stage, resulting in suppression of granulocytic precursors and the subsequent direct promotion of DC development. This is supported by earlier findings that showed impaired granulocyte formation following β-catenin activation in HSC (41). Further, constitutive DC β-catenin signaling in our study appeared to push differentiation towards mature DC subsets by depleting early progenitor pre-cDC pools. Future studies should identify the activating Wnt ligand responsible for driving DC differentiation and suppressing granulocyte formation during hematopoiesis.

Several lines of evidence indicate a role for $CD8\alpha^+$ DC in antigen cross-presentation and activation of $CD8^+$ T lymphocytes (5, 34). *Toxoplasma* is well known for its ability to elicit potent $CD8^+$ T cell responses, and cross-presentation has previously been found to play a role in MHC class I presentation to $CD8^+$ T cells during infection with this intracellular protozoan (46, 47). Therefore, it was initially surprising that there was no indication of abnormally strong $CD8^+$ T cell responses in *T. gondii*-infected $Ex3^{DC-/-}$ mice that

overexpress CD8α$^+$ DC. However, the recent discovery that the parasite directly injects a subset of secretory proteins into the host cell cytoplasm (48), as well as evidence that the majority of T cell activation is stimulated by actively infected DC (49), argues that conventional presentation rather than cross-presentation may be the dominant mechanism for CD8$^+$ T cell priming during *T. gondii* infection.

In contrast to normal CD8$^+$ T cell responses following *Toxoplasma* infection in mice with DC-specific β-catenin activation, there was a clear increase in CD4$^+$ T cell, and to a lesser extent NK cell, IFN-γ production in the mutant mice. This is of interest because CD4$^+$ and CD11b$^+$ DC, which are believed to be the most adept at activating CD4$^+$ T cells (50), were unchanged or even reduced in Ex3$^{DC-/-}$ mice. Therefore, it is most likely that increased CD4$^+$ T and NK cell IFN-γ resulted from increased splenic CD8α$^+$ DC activity, and that failure to activate CD8$^+$ T cells was due to the lack of cross-presentation. This is supported by the finding that virus-specific CD8 T cell responses were enhanced during VACV infection, which has been shown to require the cross-presentation pathway for CD8$^+$ T cell activation.

Our findings uncover for the first time a role for stabilized β-catenin signaling in promoting DC subset differentiation and activity. Based upon previous findings, it has been suggested that exploiting strategies that activate β-catenin signaling in DC might be useful in the control of inflammatory and autoimmune diseases (12, 13). Our study throws a cautionary light on this approach, showing that constitutive β-catenin signaling promotes differentiation of IRF8-dependent DC resulting in increased proinflammatory responses during protozoan and viral infection.

Supplementary Material

Refer to Web version on PubMed Central for supplementary material.

Acknowledgments

This work was supported by the NIH (AI109061, EYD; AI083405, GSY; AI110613, BDR) and a scholarship from the Cornell Vertebrate Genomics group (SBC).

We thank M. Hossain for technical assistance.

Abbreviations used in this article

BMDC	bone marrow-derived DC
cDC	conventional DC
CDP	common dendritic progenitor
CMP	common myeloid progenitor
DC	dendritic cell
GMP	granulocyte-macrophage progenitor
IRF	interferon regulatory factor

pDC	plasmacytoid DC
STAg	soluble tachyzoite antigen

References

1. Merad M, Sathe P, Helft J, Miller J, Mortha A. The dendritic cell lineage: ontogeny and function of dendritic cells and their subsets in the steady state and the inflamed setting. Annu Rev Immunol. 2013; 31:563–604. [PubMed: 23516985]
2. Belz GT, Nutt SL. Transcriptional programming of the dendritic cell network. Nat Rev Immunol. 2012; 12:101–113. [PubMed: 22273772]
3. Satpathy AT, KC W, Albring JC, Edelson BT, Kretzer NM, Bhattacharya D, Murphy TL, Murphy KM. Zbtb46 expression distinguishes classical dendritic cells and their committed progenitors from other immune lineages. Journal of Experimental Medicine. 2012; 209:1135–1152. [PubMed: 22615127]
4. Jackson JT, Hu Y, Liu R, Masson F, D'Amico A, Carotta S, Xin A, Camilleri MJ, Mount AM, Kallies A, Wu L, Smyth GK, Nutt SL, Belz GT. Id2 expression delineates differential checkpoints in the genetic program of CD8α+ and CD103+ dendritic cell lineages. EMBO J. 2011; 30:2690–2704. [PubMed: 21587207]
5. Hildner K, Edelson BT, Purtha WE, Diamond M, Matsushita H, Kohyama M, Calderon B, Schraml BU, Unanue ER, Diamond MS, Schreiber RD, Murphy TL, Murphy KM. Batf3 deficiency reveals a critical role for CD8alpha+ dendritic cells in cytotoxic T cell immunity. Science. 2008; 322:1097–1100. [PubMed: 19008445]
6. Persson EK, Uronen-Hansson H, Semmrich M, Rivollier A, Hägerbrand K, Marsal J, Gudjonsson S, Håkansson U, Reizis B, Kotarsky K, Agace WW. IRF4 transcription-factor-dependent CD103(+)CD11b(+) dendritic cells drive mucosal T helper 17 cell differentiation. Immunity. 2013; 38:958–969. [PubMed: 23664832]
7. Staal FJT, Clevers HC. WNT signalling and haematopoiesis: a WNT-WNT situation. Nat Rev Immunol. 2005; 5:21–30. [PubMed: 15630426]
8. Reya T, Duncan AW, Ailles L, Domen J, Scherer DC, Willert K, Hintz L, Nusse R, Weissman IL. A role for Wnt signalling in self-renewal of haematopoietic stem cells. Nature. 2003; 423:409–414. [PubMed: 12717450]
9. Clevers H, Nusse R. Wnt/β-catenin signaling and disease. Cell. 2012; 149:1192–1205. [PubMed: 22682243]
10. Klaus A, Birchmeier W. Wnt signalling and its impact on development and cancer. Nat Rev Cancer. 2008; 8:387–398. [PubMed: 18432252]
11. Staal FJT, Luis TC, Tiemessen MM. WNT signalling in the immune system: WNT is spreading its wings. Nat Rev Immunol. 2008; 8:581–593. [PubMed: 18617885]
12. Jiang A, Bloom O, Ono S, Cui W, Unternaehrer J, Jiang S, Whitney JA, Connolly J, Banchereau J, Mellman I. Disruption of E-cadherin-mediated adhesion induces a functionally distinct pathway of dendritic cell maturation. Immunity. 2007; 27:610–624. [PubMed: 17936032]
13. Manicassamy S, Reizis B, Ravindran R, Nakaya H, Salazar-Gonzalez RM, Wang YC, Pulendran B. Activation of β-Catenin in Dendritic Cells Regulates Immunity Versus Tolerance in the Intestine. Science. 2010; 329:849–853. [PubMed: 20705860]
14. Harada N, Tamai Y, Ishikawa T, Sauer B, Takaku K, Oshima M, Taketo MM. Intestinal polyposis in mice with a dominant stable mutation of the beta-catenin gene. EMBO J. 1999; 18:5931–5942. [PubMed: 10545105]
15. Mashayekhi M, Sandau MM, Dunay IR, Frickel EM, Khan A, Goldszmid RS, Sher A, Ploegh HL, Murphy TL, Sibley LD, Murphy KM. CD8α(+) dendritic cells are the critical source of interleukin-12 that controls acute infection by Toxoplasma gondii tachyzoites. Immunity. 2011; 35:249–259. [PubMed: 21867928]

16. Sigal LJ, Crotty S, Andino R, Rock KL. Cytotoxic T-cell immunity to virus-infected non-haematopoietic cells requires presentation of exogenous antigen. Nature. 1999; 398:77–80. [PubMed: 10078533]
17. Rudd BD, Venturi V, PDavenport M, Nikolich-Zugich J. Evolution of the antigen-specific CD8+ TCR repertoire across the life span: evidence for clonal homogenization of the old TCR repertoire. The Journal of Immunology. 2011; 186:2056–2064. [PubMed: 21248263]
18. Schneider AG, Abi Abdallah DS, Butcher BA, Denkers EY. Toxoplasma gondii triggers phosphorylation and nuclear translocation of dendritic cell STAT1 while simultaneously blocking IFNγ-induced STAT1 transcriptional activity. PLoS ONE. 2013; 8:e60215. [PubMed: 23527309]
19. Bedoui S, Prato S, Mintern J, Gebhardt T, Zhan Y, Lew AM, Heath WR, Villadangos JA, Segura E. Characterization of an immediate splenic precursor of CD8+ dendritic cells capable of inducing antiviral T cell responses. The Journal of Immunology. 2009; 182:4200–4207. [PubMed: 19299718]
20. Denkers EY, Gazzinelli RT, Hieny S, Caspar P, Sher A. Bone marrow macrophages process exogenous Toxoplasma gondii polypeptides for recognition by parasite-specific cytolytic T lymphocytes. J Immunol. 1993; 150:517–526. [PubMed: 8419484]
21. Butcher BA, Kim L, Johnson PF, Denkers EY. Toxoplasma gondii tachyzoites inhibit proinflammatory cytokine induction in infected macrophages by preventing nuclear translocation of the transcription factor NF-kappa B. J Immunol. 2001; 167:2193–2201. [PubMed: 11490005]
22. Cohen SB, Maurer KJ, Egan CE, Oghumu S, Satoskar AR, Denkers EY. CXCR3-dependent CD4+ T cells are required to activate inflammatory monocytes for defense against intestinal infection. PLoS Pathog. 2013; 9:e1003706. [PubMed: 24130498]
23. Liu K, Victora GD, Schwickert TA, Guermonprez P, Meredith MM, Yao K, Chu FF, Randolph GJ, Rudensky AY, Nussenzweig M. In vivo analysis of dendritic cell development and homeostasis. Science. 2009; 324:392–397. [PubMed: 19286519]
24. Edelson BT, KC W, Juang R, Kohyama M, Benoit LA, Klekotka PA, Moon C, Albring JC, Ise W, Michael DG, Bhattacharya D, Stappenbeck TS, Holtzman MJ, Sung S-SJ, Murphy TL, Hildner K, Murphy KM. Peripheral CD103+ dendritic cells form a unified subset developmentally related to CD8alpha+ conventional dendritic cells. Journal of Experimental Medicine. 2010; 207:823–836. [PubMed: 20351058]
25. Kashiwada M, Pham NLL, Pewe LL, Harty JT, Rothman PB. NFIL3/E4BP4 is a key transcription factor for CD8α+ dendritic cell development. Blood. 2011; 117:6193–6197. [PubMed: 21474667]
26. Tamura T, Tailor P, Yamaoka K, Kong HJ, Tsujimura H, O'Shea JJ, Singh H, Ozato K. IFN regulatory factor-4 and -8 govern dendritic cell subset development and their functional diversity. J Immunol. 2005; 174:2573–2581. [PubMed: 15728463]
27. Hacker C, Kirsch RD, Ju XS, Hieronymus T, Gust TC, Kuhl C, Jorgas T, Kurz SM, Rose-John S, Yokota Y, Zenke M. Transcriptional profiling identifies Id2 function in dendritic cell development. Nat Immunol. 2003; 4:380–386. [PubMed: 12598895]
28. Emami KH, Nguyen C, Ma H, Kim DH, Jeong KW, Eguchi M, Moon RT, Teo JL, Oh SW, Kim HY, Moon SH, Ha JR, Kahn M. A small molecule inhibitor of beta-catenin/CREB-binding protein transcription [corrected]. Proc Natl Acad Sci USA. 2004; 101:12682–12687. [PubMed: 15314234]
29. Jho EH, Zhang T, Domon C, Joo CK, Freund JN, Costantini F. Wnt/beta-catenin/Tcf signaling induces the transcription of Axin2, a negative regulator of the signaling pathway. Mol Cell Biol. 2002; 22:1172–1183. [PubMed: 11809808]
30. Fuertes Marraco SA, Grosjean F, Duval A, Rosa M, Lavanchy C, Ashok D, Haller S, Otten LA, Steiner Q-G, Descombes P, Luber CA, Meissner F, Mann M, Szeles L, Reith W, Acha-Orbea H. Novel murine dendritic cell lines: a powerful auxiliary tool for dendritic cell research. Front Immunol. 2012; 3:331. [PubMed: 23162549]
31. Raetz M, Kibardin A, Sturge CR, Pifer R, Li H, Burstein E, Ozato K, Larin S, Yarovinsky F. Cooperation of TLR12 and TLR11 in the IRF8-dependent IL-12 response to Toxoplasma gondii profilin. The Journal of Immunology. 2013; 191:4818–4827. [PubMed: 24078692]
32. Xu H, Zhu J, Smith S, Foldi J, Zhao B, Chung AY, Outtz H, Kitajewski J, Shi C, Weber S, Saftig P, Li Y, Ozato K, Blobel CP, Ivashkiv LB, Hu X. Notch-RBP-J signaling regulates the

transcription factor IRF8 to promote inflammatory macrophage polarization. Nat Immunol. 2012; 13:642–650. [PubMed: 22610140]

33. Mordue DG, Monroy F, La Regina M, Dinarello CA, Sibley LD. Acute toxoplasmosis leads to lethal overproduction of Th1 cytokines. J Immunol. 2001; 167:4574–4584. [PubMed: 11591786]
34. Haanden JM, Lehar SM, Bevan MJ. CD8(+) but not CD8(−) dendritic cells cross-prime cytotoxic T cells in vivo. J Exp Med. 2000; 192:1685–1696. [PubMed: 11120766]
35. Wilson DC, Grotenbreg GM, Liu K, Zhao Y, Frickel EM, Gubbels MJ, Ploegh HL, Yap GS. Differential regulation of effector- and central-memory responses to Toxoplasma gondii Infection by IL-12 revealed by tracking of Tgd057-specific CD8+ T cells. PLoS Pathog. 2010; 6:e1000815. [PubMed: 20333242]
36. Grover HS, Blanchard N, Gonzalez F, Chan S, Robey EA, Shastri N. The Toxoplasma gondii peptide AS15 elicits CD4 T cells that can control parasite burden. Infection and Immunity. 2012; 80:3279–3288. [PubMed: 22778097]
37. Ramirez MC, Sigal LJ. Macrophages and dendritic cells use the cytosolic pathway to rapidly cross-present antigen from live, vaccinia-infected cells. J Immunol. 2002; 169:6733–6742. [PubMed: 12471104]
38. Schiavoni G, Mattei F, Sestili P, Borghi P, Venditti M, Morse HC, Belardelli F, Gabriele L. ICSBP is essential for the development of mouse type I interferon-producing cells and for the generation and activation of CD8alpha(+) dendritic cells. J Exp Med. 2002; 196:1415–1425. [PubMed: 12461077]
39. Timm A, Grosschedl R. Wnt signaling in lymphopoiesis. Curr Top Microbiol Immunol. 2005; 290:225–252. [PubMed: 16480045]
40. Scheller M, Huelsken J, Rosenbauer F, Taketo MM, Birchmeier W, Tenen DG, Leutz A. Hematopoietic stem cell and multilineage defects generated by constitutive beta-catenin activation. Nat Immunol. 2006; 7:1037–1047. [PubMed: 16951686]
41. Scheller M, Schönheit J, Zimmermann K, Leser U, Rosenbauer F, Leutz A. Cross talk between Wnt/β-catenin and Irf8 in leukemia progression and drug resistance. Journal of Experimental Medicine. 2013; 210:2239–2256. [PubMed: 24101380]
42. Tamura T, Nagamura-Inoue T, Shmeltzer Z, Kuwata T, Ozato K. ICSBP directs bipotential myeloid progenitor cells to differentiate into mature macrophages. Immunity. 2000; 13:155–165. [PubMed: 10981959]
43. Becker AM, Michael DG, Satpathy AT, Sciammas R, Singh H, Bhattacharya D. IRF-8 extinguishes neutrophil production and promotes dendritic cell lineage commitment in both myeloid and lymphoid mouse progenitors. Blood. 2012; 119:2003–2012. [PubMed: 22238324]
44. Holtschke T, Löhler J, Kanno Y, Fehr T, Giese N, Rosenbauer F, Lou J, Knobeloch KP, Gabriele L, Waring JF, Bachmann MF, Zinkernagel RM, Morse HC, Ozato K, Horak I. Immunodeficiency and chronic myelogenous leukemia-like syndrome in mice with a targeted mutation of the ICSBP gene. Cell. 1996; 87:307–317. [PubMed: 8861914]
45. Kirstetter P, Anderson K, Porse BT, Jacobsen SEW, Nerlov C. Activation of the canonical Wnt pathway leads to loss of hematopoietic stem cell repopulation and multilineage differentiation block. Nat Immunol. 2006; 7:1048–1056. [PubMed: 16951689]
46. Goldszmid RS, Coppens I, Lev A, Caspar P, Mellman I, Sher A. Host ER-parasitophorous vacuole interaction provides a route of entry for antigen cross-presentation in Toxoplasma gondii-infected dendritic cells. Journal of Experimental Medicine. 2009; 206:399–410. [PubMed: 19153244]
47. John B, Harris TH, Tait ED, Wilson EH, Gregg B, Ng LG, Mrass P, Roos DS, Dzierszinski F, Weninger W, Hunter CA. Dynamic Imaging of CD8(+) T cells and dendritic cells during infection with Toxoplasma gondii. PLoS Pathog. 2009; 5:e1000505. [PubMed: 19578440]
48. Melo MB, Jensen KDC, Saeij JPJ. Toxoplasma gondii effectors are master regulators of the inflammatory response. Trends Parasitol. 2011; 27:487–495. [PubMed: 21893432]
49. Dupont CD, Christian DA, Selleck EM, Pepper M, Leney-Greene M, Harms Pritchard G, Koshy AA, Wagage S, Reuter MA, Sibley LD, Betts MR, Hunter CA. Parasite Fate and Involvement of Infected Cells in the Induction of CD4+ and CD8+ T Cell Responses to Toxoplasma gondii. PLoS Pathog. 2014; 10:e1004047. [PubMed: 24722202]

50. Vander Lugt B, Khan AA, Hackney JA, Agrawal S, Lesch J, Zhou M, Lee WP, Park S, Xu M, DeVoss J, Spooner CJ, Chalouni C, Delamarre L, Mellman I, Singh H. Transcriptional programming of dendritic cells for enhanced MHC class II antigen presentation. Nat Immunol. 2014; 15:161–167. [PubMed: 24362890]

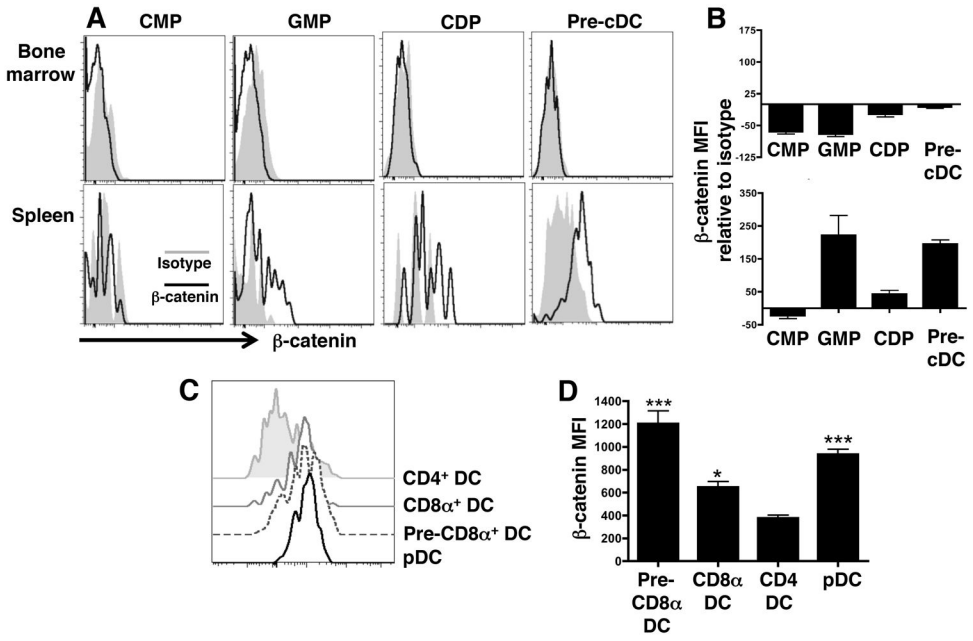

FIGURE 1.

β-catenin is upregulated in splenic DC precursors and mature DC subsets. (**A** and **B**) Flow cytometric analysis of β-catenin expression by mean fluorescent intensity (MFI) in DC precursors from the bone marrow and spleen of naïve WT mice compared to isotype control staining. The data are representative of 2 independent experiments (n=4 mice per group). (**C**) Comparison of β-catenin expression levels among splenic DC subsets by flow cytometry. (**D**) MFI of β-catenin expression among different DC subsets. Statistics are relative to β-catenin expression in $CD4^+$ DC. The data are representative of 3 independent experiments (n=5 mice per group). *, $p<0.05$; ***, $p<0.001$.

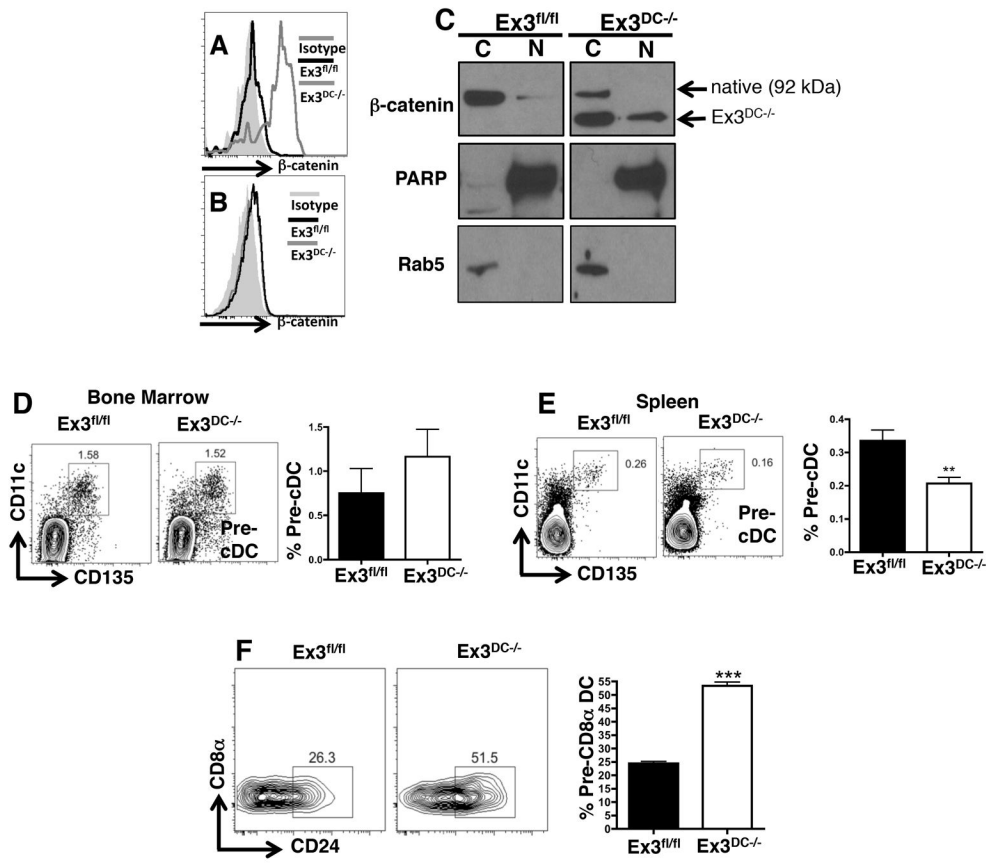

FIGURE 2.

β-catenin stabilization directs splenic DC progenitors towards CD8α$^+$ DC development. (**A**) Intracellular β-catenin expression in naïve Ex3$^{fl/fl}$ and Ex3$^{DC-/-}$ splenic CD11c$^+$ cells. (**B**) Intracellular β-catenin levels in splenic CD4$^+$ T cells isolated from Ex3$^{fl/fl}$ and Ex3$^{DC-/-}$ mice. The data show results from an individual mouse that is representative of of at least 3 experiments with 3–5 mice per group. (**C**) Western blot analysis of β-catenin in bone marrow-derived DC from Ex3$^{fl/fl}$ and Ex3$^{DC-/-}$ mice following cytoplasmic (C) and nuclear (N) fractionation. Antibodies against PARP and Rab5 were used for nuclear and cytoplasmic loading controls, respectively. The data are from 1 independent trial. (**D** and **E**) Comparison pre-cDC populations from the (**D**) bone marrow and (**E**) spleen of Ex3$^{fl/fl}$ and Ex3$^{DC-/-}$ mice by flow cytometry. Numbers in representative plots represent percentages of relevant populations within the indicated gate. Bar graphs show mean percentages plus standard error (S.E.) of relevant populations. The data represent the combination of 2 independent experiments (n=10 mice per group). (**F**) Levels of splenic pre-CD8α$^+$ DC, defined as CD11c$^+$CD8α$^-$B220$^-$CD24$^+$, in Ex3$^{fl/fl}$ and Ex3$^{DC-/-}$ mice by flow cytometry. The data are representative of 3 independent experiments, each involving 4–5 mice per group. **, $p<0.01$; ***, $p<0.001$.

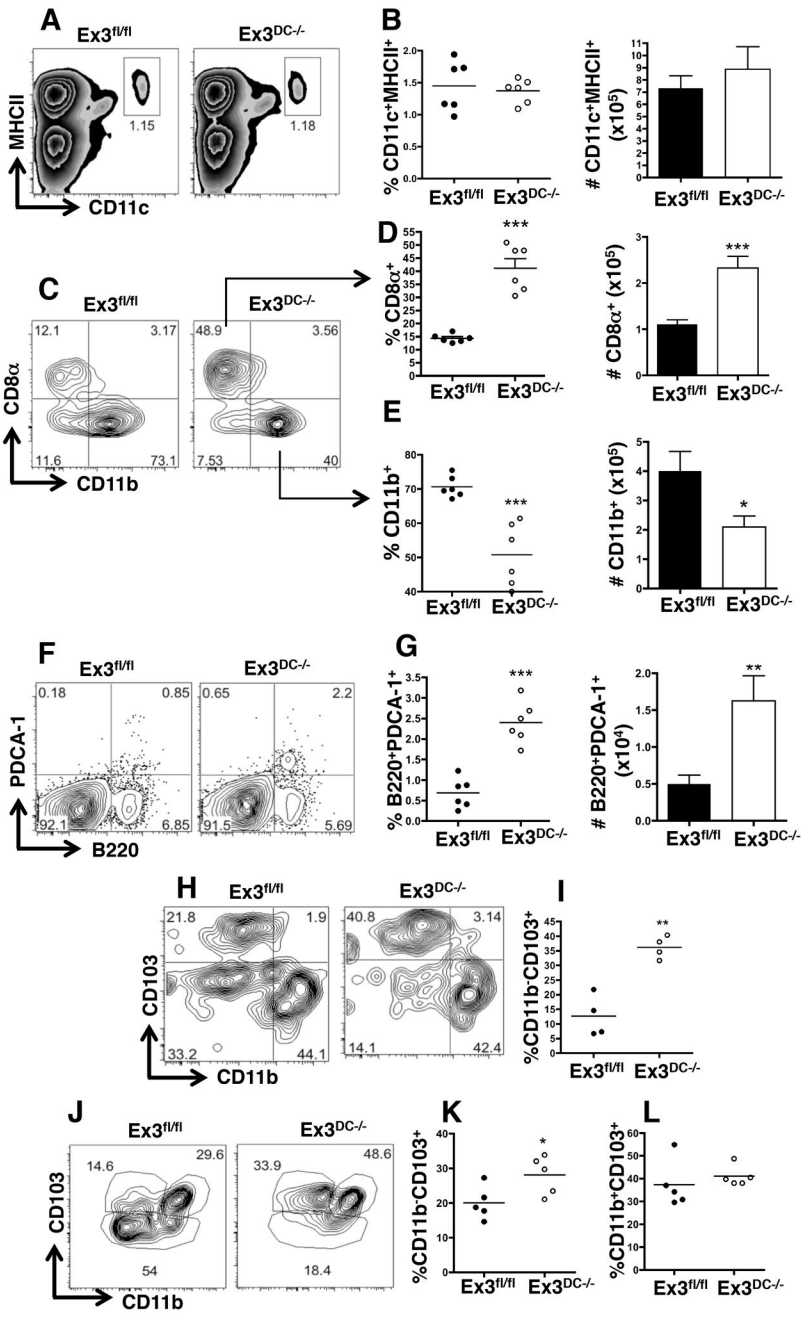

FIGURE 3.

β-catenin stabilization expands splenic CD8α$^+$ and plasmacytoid DC populations. (**A–G**) Mature DC subset analysis of naïve Ex3$^{fl/fl}$ and Ex3$^{DC-/-}$ splenocytes by flow cytometry. (**A** and **B**) Percentage and total number of CD11c$^+$ cells in Ex3$^{fl/fl}$ and Ex3$^{DC-/-}$ spleens. (**C–E**) Percentage and total number of (**C** and **D**) CD8α$^+$ DC and (**C** and **E**) CD11b$^+$ DC in naïve Ex3$^{fl/fl}$ and Ex3$^{DC-/-}$ spleens. The data are representative of at least 3 independent experiments (n=3–5 mice per group). (**F** and **G**) Percentage and total number of B220$^+$PDCA-1$^+$ plasmacytoid DC in naïve Ex3$^{fl/fl}$ and Ex3$^{DC-/-}$ spleens. (**H** and **I**) Mature DC subset analysis of naïve Ex3$^{fl/fl}$ and Ex3$^{DC-/-}$ lung tissue by flow cytometry. (**H**) Plots

from representative mice and (**I**) percentage of $CD103^{+}CD11b^{-}$ lung DC for multiple mice are shown. (**J–L**) Mature DC subset analysis of naïve $Ex3^{fl/fl}$ and $Ex3^{DC-/-}$ intestinal lamina propria by flow cytometry. (**J**) Plots from representative mice and percentages of (**K**) $CD103^{+}CD11b^{-}$ and (**L**) $CD103^{+}CD11b^{+}$ intestinal DC for multiple mice are shown. Dots in relevant graphs represent results from individual mice. Bar graphs display means and standard errors of individual mice. The data are representative of at least 2 independent experiments (n=3–5 mice per group). *, $p<0.05$; **, $p<0.01$; ***, $p<0.001$.

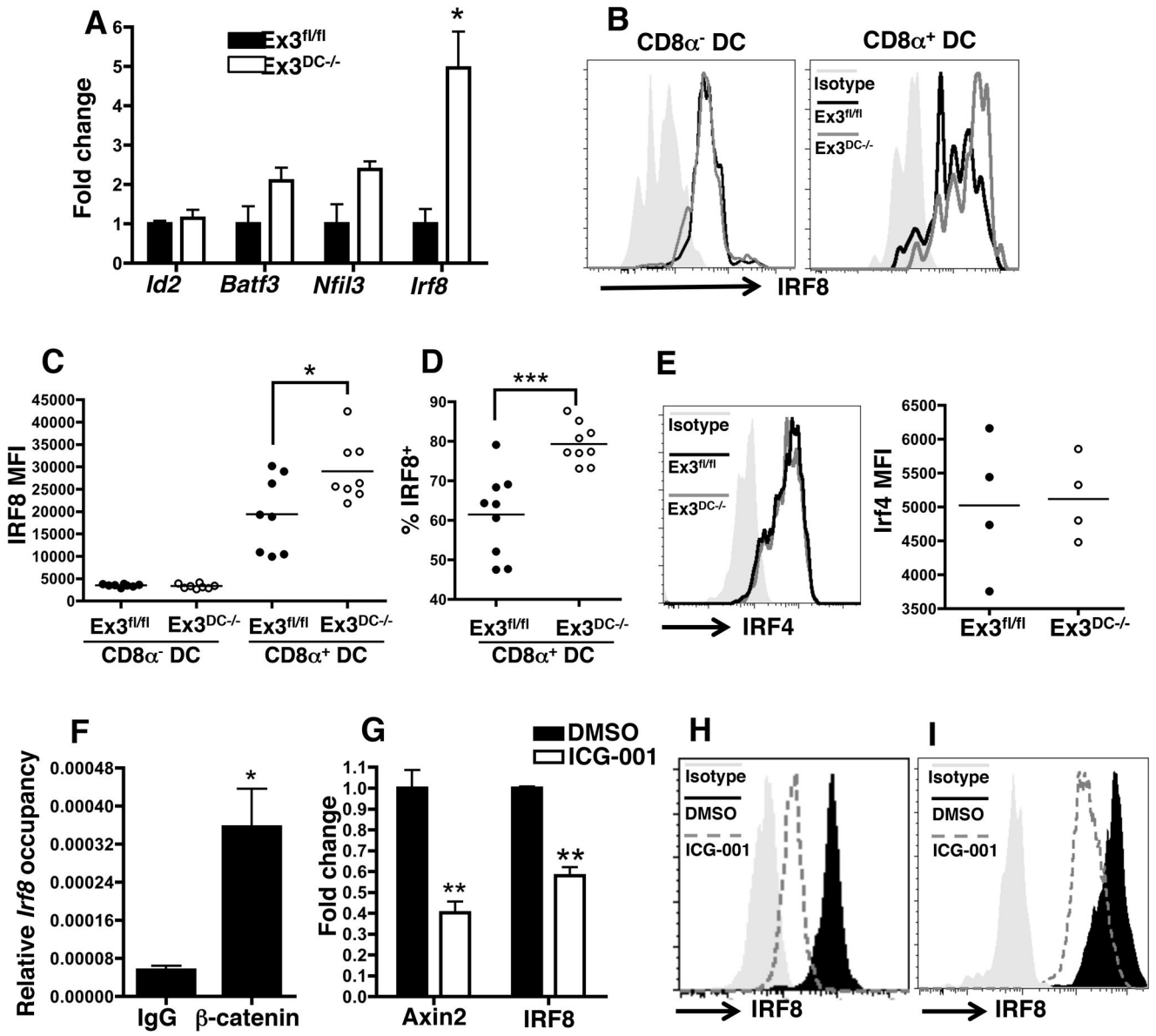

FIGURE 4.

β-catenin signaling controls *Irf8* expression. (**A**) Semi-quantitative PCR analysis of *Nfil3*, *Batf3*, *Id2*, and *Irf8* mRNA in CD11c$^+$ splenocytes magnetically purified from naïve Ex3$^{fl/fl}$ and Ex3$^{DC-/-}$ mice. mRNA levels were normalized to GAPDH. The data are representative of 2 independent experiments (n=2–3 mice per group) (**B**) Representative flow cytometric plots of IRF8 expression by Ex3$^{fl/fl}$ and Ex3$^{DC-/-}$ CD8α$^-$ and CD8α$^+$ splenic DC. (**C**) MFI of IRF8 within Ex3$^{fl/fl}$ and Ex3$^{DC-/-}$ CD8α$^-$ and CD8α$^+$ DC and (**D**) the percent of CD8α$^+$ DC expressing IRF8 are shown. Dots represent results from individual mice. The data are the combined results of 2 experiments, and the experiment was independently performed at least 3 times (n=4–5 mice per group). (**E**) Representative FACS plot of IRF4 expression and IRF4 MFI in Ex3$^{fl/fl}$ and Ex3$^{DC-/-}$ CD11c$^+$ splenocytes. The data are representative of 3 independent experiments (n=4 mice per group). (**F**) Chromatin immunoprecipitation of

naïve $Ex3^{DC-/-}$ Flt3L DC cultures with control IgG or β-catenin antibody followed by quantitative PCR to determine *Irf8* promoter occupancy. DNA levels were normalized to 1% input chromatin. The data are representative of 2 independent experiments. (**G**) Quantitative PCR analysis of *Axin2* and *Irf8* gene expression in BMDC following 5 hr culture with DMSO or ICG-001. Fold change is relative to DMSO control. The data are from one independent trial. (H and I) Intracellular expression of IRF8 and β-catenin following ICG-001 treatment of BMDC (H) or MutuDC1940 cells (I). The data are representative of 2 (MutuDC1940 cells) and 4 (BMDC) independent experiments with 3 replicates per treatment per experiment. *, $p<0.05$; **, $p<0.01$; ***, $p<0.001$.

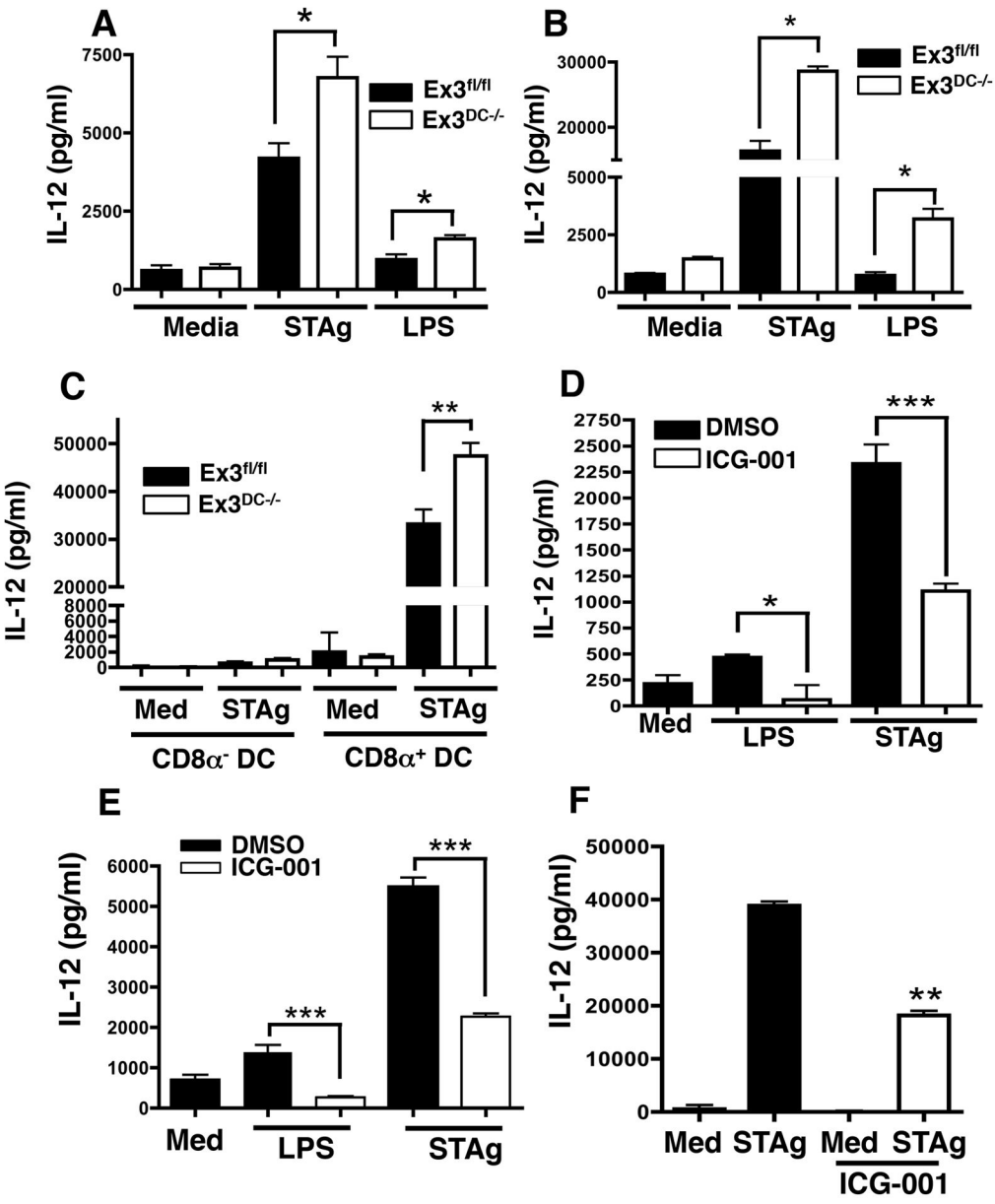

FIGURE 5.

β-catenin stabilization enhances IL-12 production by CD8α$^+$ DC. (**A**) IL-12p40 production by naïve Ex3$^{fl/fl}$ and Ex3$^{DC-/-}$ splenocytes stimulated in vitro with LPS, STAg, or media control measured by ELISA. (**B**) IL-12p40 production by splenic CD11c$^+$ DC magnetically purified from Ex3$^{fl/fl}$ and Ex3$^{DC-/-}$ mice stimulated in vitro with LPS, STAg, or media control measured by ELISA. (**C**) IL-12p40 production by CD8α$^+$ and CD8α$^-$ DC DC purified from naïve Ex3$^{fl/fl}$ and Ex3$^{DC-/-}$ splenocytes following in vitro stimulation with media or STAg for 48 hr measured by ELISA. (**D**) IL-12p40 secretion by Ex3$^{fl/fl}$ splenocytes pre-treated with ICG-001 for 5 hr and then stimulated overnight with LPS or STAg measured by ELISA. (**E**) IL-12p40 production by splenocytes (10^6) from Ex3$^{DC-/-}$ mice cultured for 5 hr with 5 μM ICG-001 or DMSO and then stimulated with media, LPS

(100 ng/ml), or STAg (25 μg/ml) overnight. (**F**) IL-12p40 production by MutuDC1940 cells (10^5) pre-treated with 20 μM ICG-001 or DMSO for 2 hr and then stimulated with media or STAg (25 μg/ml) overnight. The data are representative of at least 3 (A, F) and 2 (B–E) independent experiments, each involving 3–5 mice per group, except (C), which used pooled samples from 3 mice per experiment. *, $p<0.05$; **, $p<0.01$; ***, $p<0.001$.

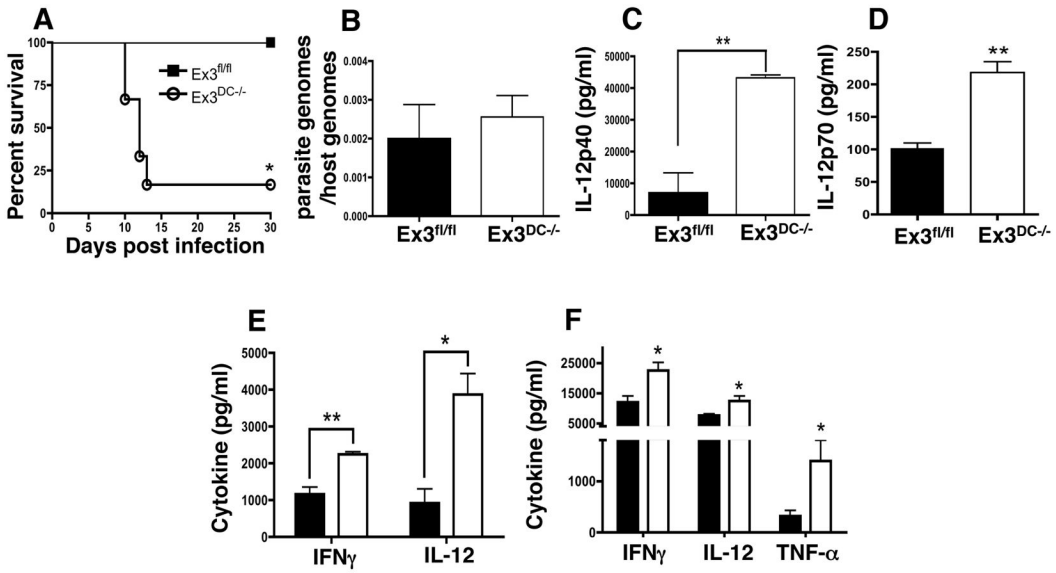

FIGURE 6.

Constitutive DC β-catenin signaling increases the proinflammatory cytokine response to *Toxoplasma*. (**A**) Survival of $Ex3^{fl/fl}$ and $Ex3^{DC-/-}$ mice following i.p. infection with *Toxoplasma* Type II strain ME49 (25 cysts) (n=4–6 mice per group). The data are representative of at least 3 experiments. (**B**) Quantitative PCR amplification of parasite (B1 gene) and host DNA (ASL gene) isolated from $Ex3^{fl/fl}$ and $Ex3^{DC-/-}$ spleens 9 days post-infection. Parasite load is displayed as a ratio of parasite genomes to host genomes (n=3–4 mice per group). (**C**) IL-12p40 production by $CD11c^{+}$ DC magnetically separated from Day-6 post-infection $Ex3^{fl/fl}$ and $Ex3^{DC-/-}$ splenocytes and cultured overnight without additional stimulation (n=3 mice per group). (**D**) IL-12p70 production by bulk splenocytes from Day-6 post-infection $Ex3^{fl/fl}$ and $Ex3^{DC-/-}$ mice (n=3 mice per group). The data are representative of 2 independent experiments. (**E**) IL-12p40 and IFN-γ production by splenocytes from Day-10 post-infection $Ex3^{fl/fl}$ and $Ex3^{DC-/-}$ mice cultured for 72 hr without additional stimulation (n=3–5 mice per group). The data are representative of 3 independent experiments. (**F**) IL-12p40, IFN-γ, and TNF-α levels in serum collected from Day-9 post-infection $Ex3^{fl/fl}$ and $Ex3^{DC-/-}$ mice (n=3–5 mice per group). The data are representative of 2 independent experiments. The means and S.E. of individual mice are shown. *, $p<0.05$; **, $p<0.01$.

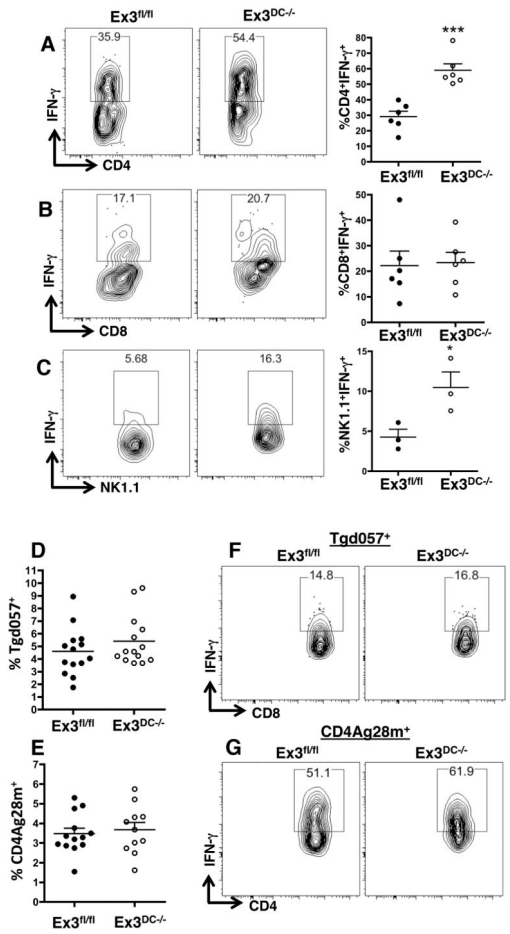

FIGURE 7.

$CD4^+$ T cells and NK cells, but not $CD8^+$ T cells, overproduce IFN-γ following *Toxoplasma* infection in mice with constitutive DC β-catenin signaling. (**A–C**) Intracellular flow cytometric analysis of IFN-γ production by (**A**) $CD4^+$ T cells, (**B**) $CD8^+$ T cells, and (**C**) NK cells from Day 9 *T. gondii*-infected $Ex3^{fl/fl}$ and $Ex3^{DC-/-}$ spleens following 4 hr of PMA and ionomycin stimulation in the presence of Brefeldin-A. Shown are representative contour plots of individual mice and the mean ± standard error of IFN-γ levels from multiple mice. The data are representative of 3 independent experiments (CD4 and CD8) and 1 (NK) experiment. (**D** and **E**) Quantification of *Toxoplasma*-specific (**D**) $Tgd057^+CD8^+$ T cells and (E) $CD4Ag28m^+CD4^+$ T cells. Means and standard errors of individual mice are shown, and each dot represents a single mouse. (**F** and **G**) IFN-γ levels expressed by tetramer-positive $CD8^+$ (**F**) and $CD4^+$ (**G**) T cells following 4 hr of culture with PMA, ionomycin, and Brefeldin-A. The data are representative of 3 independent experiments (n=3 mice per group). *, $p<0.05$; ***, $p<0.001$.

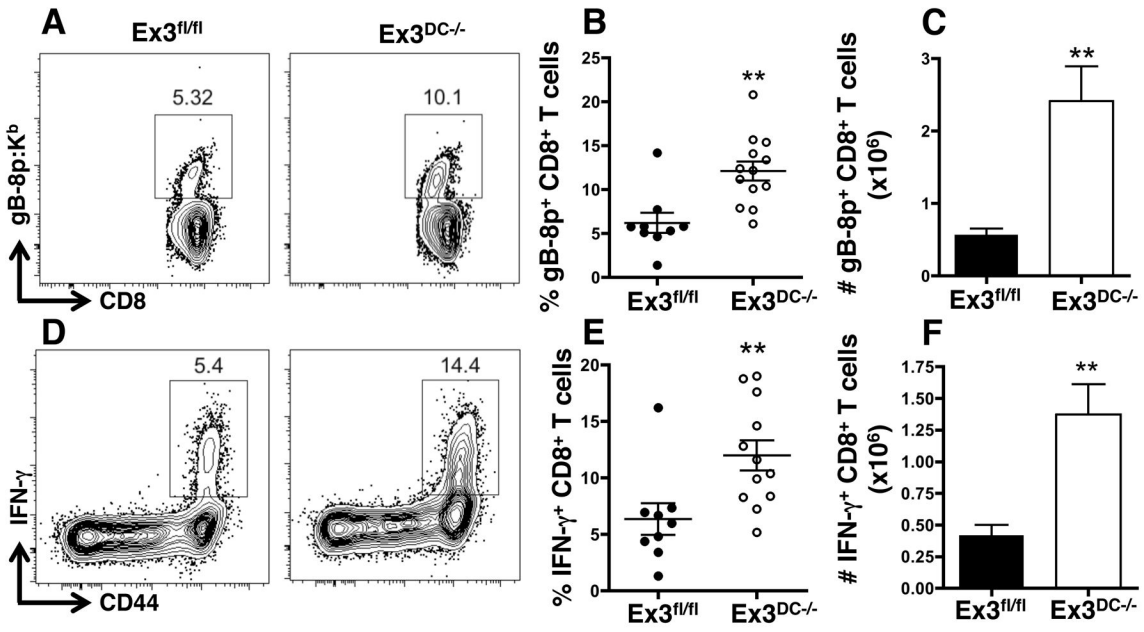

FIGURE 8.

β-catenin stabilization promotes activation of antigen-specific $CD8^+$ T cells during viral infection. (A–C) Quantification of gB-8p-specific $CD8^+$ T cells in $Ex3^{fl/fl}$ and $Ex3^{DC-/-}$ spleens 6 days post-VACV-gB infection. (**A**) Representative plots of MHCI-restricted gB-8p:K^b tetramer-positive $CD8^+$ T cells, and (**B**) percentage and (**C**) total number of gB-8p:$K^{b+}CD8^+$ T cells. (D–F) IFN-γ production by gB-8p-specific $CD8^+$ T cells in $Ex3^{fl/fl}$ and $Ex3^{DC-/-}$ spleens 6 days post-VACV-gB infection. (**D**) Representative plots of $CD8^+CD44^+$IFN-γ^+ T cells following gb-8p restimulation of splenocytes, and (**E**) percentage and (**F**) total number of gB-8p-specific $CD8^+CD44^+$IFN-γ^+ T cells. The data shown are the combination of 2 independent experiments (n=9–13). **, $p<0.01$.